

Ingeniería, investigación y tecnología

ISSN: 1405-7743 ISSN: 2594-0732

Facultad de Ingeniería, UNAM

Flores-Fuentes, Allan Antonio; Pérez-Martínez, José Arturo; García-Mejía, Juan Fernando; Rossano-Díaz, Iván Osvaldo; Torres-Reyes, Carlos Eduardo Design and simulation of a resonant full-bridge multicell power inverter for high-voltage applications Ingeniería, investigación y tecnología, vol. XIX, no. 3, 2018, July-September, pp. 245-254 Facultad de Ingeniería, UNAM

DOI: https://doi.org/10.22201/fi.25940732e.2018.19n3.021

Available in: https://www.redalyc.org/articulo.oa?id=40458315001



Complete issue



Journal's webpage in redalyc.org



Scientific Information System Redalyc

Network of Scientific Journals from Latin America and the Caribbean, Spain and Portugal

Project academic non-profit, developed under the open access initiative

Ingeniería Investigación y Tecnología volumen XIX (número 3), julio-septiembre 2018 245 -254

ISSN 2594-0732 FI-UNAM artículo arbitrado

Recibido: 13 de enero de 2016, Reevaluado: 24 de agosto de 2017, Aceptado: 23 de octubre de 2017

Attribution-NonCommercial-NoDerivatives 4.0 International (CC BY-NC-ND 4.0) license

DOI. http://dx.doi.org/10.22201/fi.25940732e.2018.19n3.021





# Design and simulation of a resonant full-bridge multicell power inverter for high-voltage applications

Diseño y simulación de un inversor multicelular de potencia resonante en puentecompleto para aplicaciones de alto voltaje

Flores-Fuentes Allan Antonio

Universidad Autónoma del Estado de México UAEMex

E-mail: aafloresf@uaemex.mx Pérez-Martínez José Arturo

Universidad Autónoma del Estado de México UAEMex

E-mail: japerezm@uamex.mx

García-Mejía Juan Fernando

Universidad Autónoma del Estado de México UAEMex

E-mail: fgarciam@uaemex.mx

Rossano-Díaz Iván Osvaldo

Universidad Autónoma del Estado de México UAEMex

E-mail: iorossanod@uaemex.mx Torres-Reyes Carlos Eduardo

Universidad Autónoma del Estado de México UAEMex

E-mail: cetorresr@uaemex.mx

### **ABSTRACT**

The design and simulation of a Full-Bridge Flying-Capacitor Multilevel-Inverter (FB-FCMI) for high-voltage applications are presented. The power inverter topology consists of two legs: each one with three commutation cells, six switches and two flying-capacitors. The proposed control system provides twelve square signals for all switches that compose the inverter, which is driven at a commutation frequency  $f_{SW} \approx 6.66 \text{ kHz}$ . The output frequency  $f_{0}$ , is equal to three times the commutation frequency. The inductor and capacitor in the resonant-circuit design is calculated based on  $f_0$ , which depends on the number of cells, N. The goal of the proposed inverter design is to demonstrate that, the output frequency increases as rate of  $f_0 = N \cdot f_{SW}$ . In order to show the effect of the increase in the number of cells, a resonant power inverter is designed and simulated, first with three and then with six switching cells, at  $f_0 = 20$  kHz. Finally, the FB-FCMI is connected to the primary winding of the high-voltage transformer, while the secondary is coupled to a Dielectric Barrier Discharge reactor represented by its electrical model, to generate an electrical discharge in helium.

Keywords: Multilevel-inverter, full-bridge, resonant-circuit, dielectric barrier discharge, electrical model.

### RESUMEN

Se presenta el diseño y simulación de un Inversor Multinivel de Capacitores Flotados (FB-FCMI, por sus siglas en inglés) en puente completo para aplicaciones de alto voltaje. La topología del inversor de potencia consiste en dos ramas, cada una con tres células de conmutación, seis interruptores y dos condensadores flotados. El sistema de control proporciona doce señales cuadradas para todos los interruptores que componen el inversor, que se opera a frecuencia de conmutación  $f_{SW} \approx 6.66$  kHz. La frecuencia de salida es  $f_{OV}$ y es igual a tres veces la frecuencia de conmutación. El diseño del inductor y condensador del circuito resonante se calcula con base en f<sub>or</sub> que está en función del número de células, N. El objetivo del diseño del inversor propuesto es demostrar que, la frecuencia de salida incrementa en proporción de  $f_0 = N \cdot f_{SW}$ . A fin de que se observe el efecto por el incremento en el número de células, un inversor resonante de potencia se diseña y simula, primero con tres y después con seis células de conmutación, a  $f_0 = 20$  kHz. Finalmente, el FB-FCMI se conecta al primario de un transformador de alto voltaje, mientras que el secundario se acopla a una descarga de barrera dieléctrica para generar una descarga eléctrica en helio.

Descriptores: Inversor multicelular, puente-completo, circuito resonante, descarga de barrera dieléctrica, modelo eléctrico.

#### Introduction

After its emergence in the the 90<sup>th</sup> by Meynard and Foch, applications of the Flying Capacitor Multicell Inverters (FCMI) has been continuously growing, leading to a wide study in the different areas of the knowledge (Meynard *et al.*, 2002). A considerable amount of literature has been published concerning about this kind of static power converter topology on industrial applications, for instance: STATCOM<sup>TM</sup> transport trains active filters to eliminate total harmonic distortion THD, cd to cd and cd to ca power converters, and more recently in Eolic conversion energy (Rodriguez *et al.*, 2012; Abu *et al.*, 2010; Fernao *et al.*, 2012).

Precedent studies about a Three Cell Flying Capacitor Inverter in half-bridge, coupled in an electrical model of a Dielectric Barrier Discharge (DBD) are presented by (Flores et al., 2009). A simulation of the electrical model is used in order to estimate the experimental results at different gas discharges, and operation frequency about 12.5 and 47 kHz implementing different commutation strategies. Nevertheless, these simulations results are limited to half-bridge and three cells. Previous works of the FCMI show a full-bridge configuration applied as electrical source in DBD applications operating at 10-20 kHz (López et al., 2015) and 12.5-50 kHz (Péña et al., 2017). In these works, experimental and simulation results show an agreement application implementing this kind of multicell inverter topology operating at high frequency.

From the perspective of FCMI technology design, switching coupling, command signal generator system and high frequency semiconductor drivers, are the considerable disadvantages, not only because specialized components are required, but also power losses and technological limitations. In fact, this kind of power inverter is usually implemented at low frequency (Zhe *et al.*, 2009; Rodriguez *et al.*, 2012; Tolbert *et al.*, 2000; Samir *et al.*, 2010).

Multicell Converters were developed in order to satisfy the electrical characteristics of high voltage and current, by Voltage Source Inverter or Current Source Inverter respectively, and more recently the high frequency operation in the order of hundreds and thousands of Hertz. In addition, the operation frequency in the FCMI is given by  $f_0 = N \cdot f_{\rm SW}$  where  $f_{\rm SW}$  is the commutation frequency; the same that semiconductor devices operation, and N is the number of cells configured like one leg in the FCMI structure. That property bringforward an intrinsic characteristic not commonly used in the typical static converters, so  $f_0$  is proportionally N times than  $f_{\rm SW}$  and that statement is an advantage, ta-

king in account that semiconductor devices, like Thyristors, GTOs and power BJTs operates at low frequency in the order of some kilo-Hertz at tens to hundreds volts-amperes. In counterpart, MOSFET and IGBT devices operates about tens to hundreds of kilo-Hertz at some tens volts-amperes (Hirofumi, 2009). That characteristics voltage-current and frequency is a restriction to choose the semiconductor device, because the more voltage and current is needed the frequency interval of work is reduced and vice versa (Loren, 2003). In the other hand, that statement is solved by using the FCMI. First, its main property consists in distribute the total voltage (VSI) or current (CSI) in the total number of cells N and when the FCMI operates at Fundamental Frequency (F-F) strategy the output operation frequency  $f_0$  is given by  $f_0 = N \cdot f_{SW}$  where  $f_{SW}$  is the switching frequency equal to the F-F. So, both characteristics are used in order to overcome the above-mentioned disadvantages.

Moreover, until few decades ago the main disadvantage of the FCMI is their complexity: they require a great number of power devices and a rather complex command firing-circuit made by analog-digital circuits. However, the current technology based on micro-controllers, Digital Signal Processor (DSP), Field Program Gate Array (FPGA), and other technologies like Arduino® or Raspberry™ has allowed the higher processing capacity in the control design with any technique implemented such as; Simple Square Wave (SSW) or Fundamental Frequency (F-F) and Pulse Wide Modulation (PWM) commonly implemented in the strategy control for FCMI (Holmes and Lipo, 2003; Rodriguez et al., 2002). The advantage to implement PWM topologies is the reducing of the Total Harmonic Distortion (THD) but as consequence, large protection circuits (dv/dt or di/dt) are required in order to help the commutation semiconductors, and so the losses increase (Aguillón et al., 2004).

Considering the above mentioned characteristics about control implementation, the proposed FB-FCMI implements an F-F strategy and as a result of the command firing-signals it produces a typical square waveform output  $u_0$  at frequency  $f_0 = N \cdot f_{\text{SW}}$  moreover due to  $f_{\text{SW}}$  is N times lesser than  $f_0$ , hence the commutation losses decrease. Actually, that property is not commonly applied on this kind of static converters, but nevertheless, on this work this feature is improved not only in order to reduce the switching frequency and complexity of the command signals implementation, but also the goal of the RLC circuit series with the FB-FCMI achieves a resonant operation.

As a contribution to operate the FB-FCMI in resonant mode converter, the design and simulation results

are shown. The calculus of either,  $L_0$  and  $C_0$  resonant elements, is presented. Finally, the high voltage application is presented by implementing an electrical model of one dielectric barrier discharge (DBD). The simulation results show the implementation of the FB-FCMI operating at 20 kHz in resonant mode in order to drive a dielectric barrier discharge in helium.

### SIMULATION DESIGN

FULL-BRIDGE FLYING CAPACITOR MULTICELL INVERTER TOPOLOGY

A resonant FB-FCMI coupled to DBD electrical model is shown in Figure 1. The inverter is constituted by six commutation cells (three upper-leg and three lower-leg), each cell is composed by two complementary MOSFET [M1, M1'], [M2, M2'], [M3, M3'], [M4, M4'], [M5, M5'] and [M6, M6'] every one with its antiparallel diode, there is a flying capacitor  $C_p$ , where p is the position of cell in upper-leg and  $C_p'$  in lower-leg.

The flying capacitor voltages  $V_{CI}=V_{CI}$  and  $V_{C2}=V_{C2}$  are defined by;  $V_{Cp,Cp'}=(\rho/N)\cdot V_{DC}$  where p is the position of the cell in the structure and N is the number of total cells. Also, the blocking voltage in the MOSFETs is estimated by  $V_{MN,MN'}=(V_{DC}/N)$  and the average current is;  $I_{kavg}=T_{on}/T\cdot I_S$  where  $T_{on}$  is the turn-on period, T is the total period and  $I_S$  is the supply current (Meynard et al., 2002).

The operation of FB-FCMI is achieving an equal distribution of the total voltage in the blocking-state MOS-

FET. This occurs when flying-capacitors are charged at;  $V_{C1,C1'} = V_{DC} / 3$  and  $V_{C2,C2'} = 2V_{DC} / 3$ , considering as ideal voltage source. The accurate MOSFET firing commutation pulses involves that C1=C1' and C2=C2', and that condition guarantees the appropriate voltage, and as result; the output voltage  $u_0(t)$  operating at output frequency  $f_0 = 3 \cdot f_{sw}$  or  $T_0 = T_{sw} / 3$  Figure 2 shows tree representative commutation pulses  $[S_1, S_2, S_3]$  provided to MOSFET M1, M2 and M3, signals are in phase shift  $120^\circ$  and  $240^\circ$  respectively, the main voltages are presented like; output  $v_0(t)$ , referenced to upper-leg  $v_W(t)$  and lower-leg  $v_V(t)$ . So, because of the voltage difference between  $v_W(t)$  and  $v_V(t)$  is made by  $v_0(t)$ .

### THE RESONANT RLC SERIES COUPLED TO FB-FCMI

As Figure 1 shows, a Dielectric Barrier Discharge electrical model is coupled to FB-FCMI. Then, the equivalent circuit can be considering by a resonant RLC series circuit. Figure 3 shows a resonant RLC series circuit determinate by the inductance  $L_{\rm C}$  primary winding of high voltage transformer and the secondary winding capacitance presented in the primary one as  $C_{\rm C}$ . The analysis of  $L_{\rm C}$ – $C_{\rm C}$  values is presented in order to get the resonant operation of the FB-FCMI.

The *RLC* series circuit of the Figure 3 is supplied by the voltage  $v_0(t)$ . Then, the total impedance  $Z_T$  obtained in frequency domain is given by

$$Z_T = R + j\omega L + \frac{1}{j\omega C} \tag{1}$$

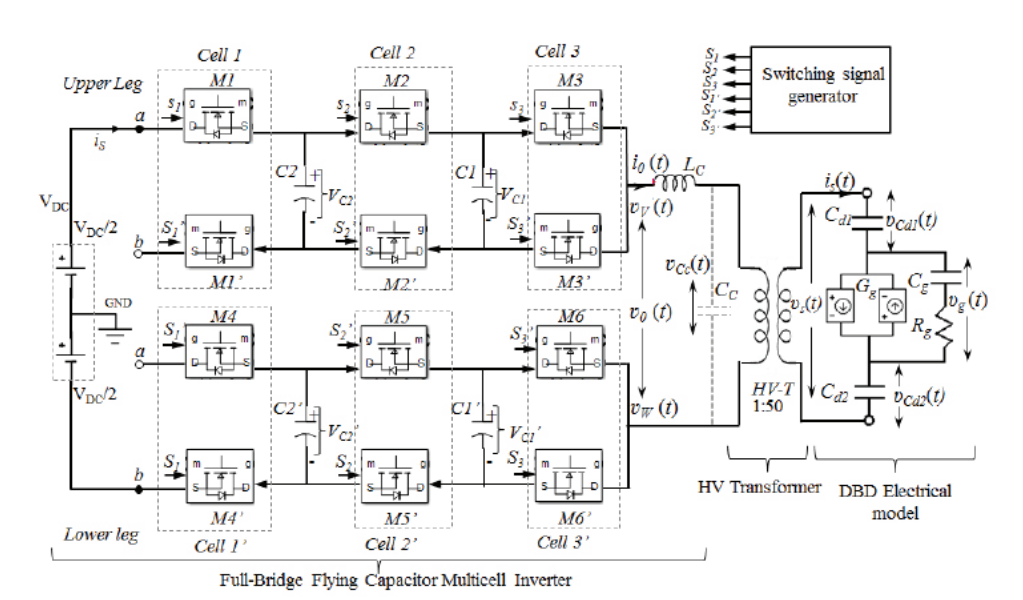


Figure 1. Scheme of a three cell resonant FB-FCMI coupled to DBD electrical model

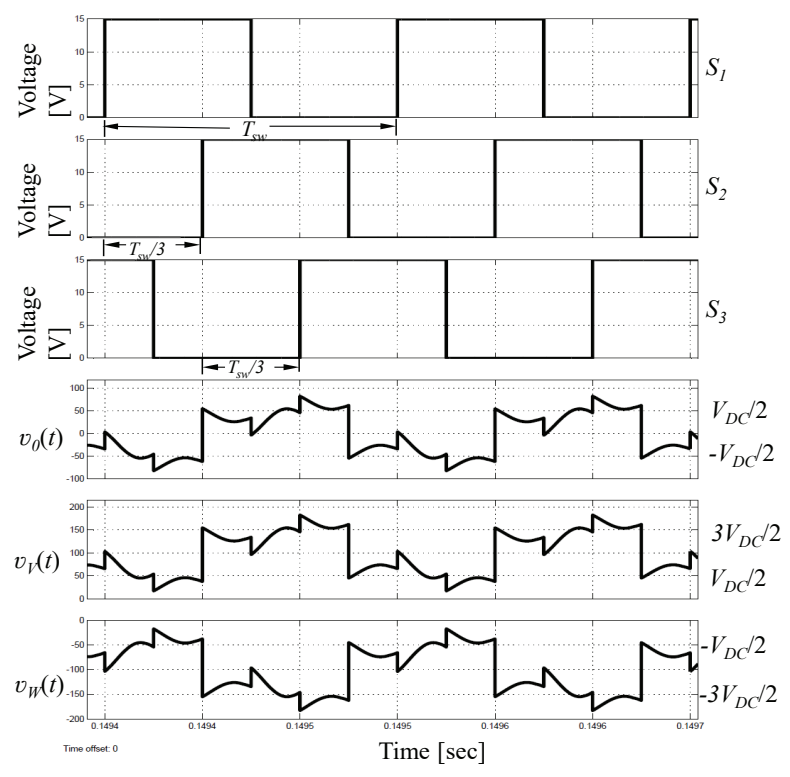


Figure 2. FB-FCMI output voltage  $\upsilon_0(t)$ , upper-leg  $\upsilon_{V}(t)$  and lower leg  $\upsilon_{W}(t)$ ; as a result of accurate commutation strategy  $[S_1, S_2, S_3]$ 

Figure 3. A resonant RLC series circuit

where  $\omega = 2\pi f$  is the angular frequency and f is the linear frequency output  $f_0$ . The total impedance for the  $n^{th}$  frequency component

$$Z_{T}(jn\omega) = \frac{1}{n\omega C} \left[ n\omega CR + j \left( n^{2}\omega^{2}LC - 1 \right) \right]$$
 (2)

Then, the magnitude and angle impedance values for the  $n^{th}$  harmonic are defined as

$$||Z_{T}(jn\omega)|| = \frac{1}{n\omega C} \sqrt{(n\omega CR)^{2} + (n^{2}\omega^{2}LC - 1)^{2}}$$
(3)

$$\theta = \arctan\left(\frac{n^2 \omega^2 LC - 1}{n\omega CR}\right) \tag{4}$$

Also, the voltage  $u_0(t)$  is a square signal provided by the FB-FCMI at the resonant RLC series circuit in Fourier term

Also, the voltage 
$$u_0(t)$$
 is a square signal provided by the

where  $V_m = V_{DC}/3$  is the maximum amplitude to the output square voltage, considering only the n odd values. So, using Ohm law to obtain the output current  $i_0(t)$  based on (2) and (5) then

$$i_0(t) = \frac{4Vm}{\pi} \left[ \sum_{n=1}^{\infty} \frac{wC \sin(nwt - \theta)}{\sqrt{(nwCR)^2 + (n^2w^2LC - 1)^2}} \right]$$
 (6)

In an ideal resonant *RLC* series circuit the  $i_0(t)$  flow from R to L without losses, but the capacitor voltage is in phase shifting  $-\pi/2$  radian, therefore the capacitor voltage  $u_{c}(t)$  is

$$u_{C}(t) = \frac{4Vm}{n\pi} \left[ \sum_{n=1}^{\infty} \frac{\sin(n\omega - \theta - \pi/2)}{\sqrt{(n\omega CR)^{2} + (n^{2}\omega^{2}LC - 1)}} \right]$$
(7)

Then, the total voltage gain  $A_u=u_c(t)/u_0(t)$  and angle, considering the  $n^{th}$  harmonic is

$$u_0(t) = \frac{4Vm}{\pi} \left[ \sum_{n=1}^{\infty} \frac{1}{n} \sin(n\omega) \right]$$
 (5)  $A_u(t) = \frac{1}{jwnCR + (1 - n^2w^2LC)}$ 

Finally, the transfer function magnitude  $\|A_u\|$  and angle  $\theta$  in term of quality factor Q at resonant angular frequency  $\omega_0$  are

$$||A_u|| = \frac{1}{\sqrt{\frac{1}{Q^2} + \left(1 - \frac{\omega^2}{\omega_0^2}\right)}}$$
 (9)

$$\theta = \arctan \left[ Q \left( \frac{\omega^2}{\omega_0^2} - 1 \right) \right] \tag{10}$$

where  $\omega_0^2 = 1/LC$  y  $Q = 1/\omega CR$ 

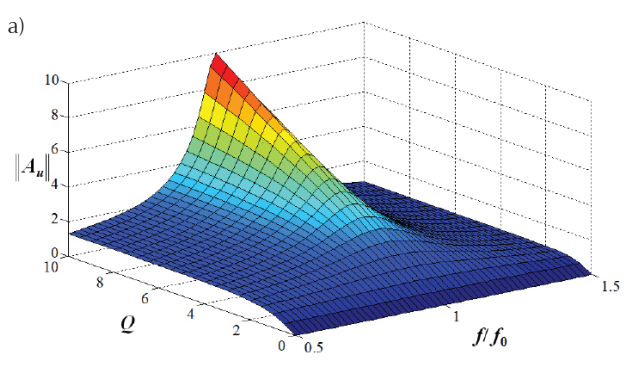
By means (9) and (10) is possible to know the magnitude  $\|A_u\|$  and angle  $\theta$ , as function of parameters Q and factor  $f/f_0$ , so the RLC series circuit is resonance mode when both frequencies either  $\omega/\omega_0$  or  $f/f_0$  are the same. Hence, two work conditions fulfill as:

- a) Maximum gain voltage  $v_0(t)/v_0(t)$ , and
- b) The output current  $i_0(t)$  and voltage  $v_0(t)$  are in same phase when Q is maximum, as Figure 4a and 4b shown respectively.

Figure 5 shows the simulation results of the FB-FC-MI obtained with SIMULINK/MATLAB®, the voltage  $v_R(t)$  and current  $i_0(t)$  values are in the same angle phase  $\phi$ =0 at  $f/f_0$  condition. Otherwise, Figure 6 shows the voltages in  $v_R(t)$ ,  $v_C(t)$  and  $v_0(t)$  at resonant condition, the waveforms evidence the statement  $f_0$ =3  $f_{sw}$ ; because the output frequency in R or C passive electrical components is  $f_0$ ≈20 kHz, three times more than commutation frequency  $f_{sw}$ ≈6.66 kHz in the voltage  $v_0(t)$ .

The increasing of the output frequency  $f_0$  is a natural property and benefit of the FB-FCMI when it operates at Fundamental Frequency, so not only is an advantage in order to increases the frequency N times but also overcomes the disadvantage of commutation losses at frequency  $f_{sv}$ . Thus, the MOSFET devices operate at  $f_{sv}$  the commutation losses are reduced, and as consequence snubber circuit protection versus voltage dv/dt and current di/dt are diminished.

Figure 7a shows the voltage  $V_{MN}(t)$  and current  $I_{MN}(t)$  through the MOSFET at Zero-Current Switching. The ZCS is when the current through a switch is reduced to significantly zero amperes prior to when the switch is being turned either on or off. It is due to RLC resonant circuit operation. Therefore, the advantage is the consi-



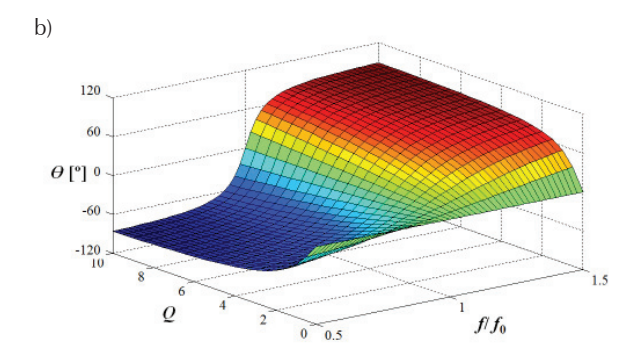


Figure 4. a) Voltage gain magnitude  $\|A_u\|$  and b) Angle  $\theta$ ; as function of quality factor Q and  $f/f_0$ 

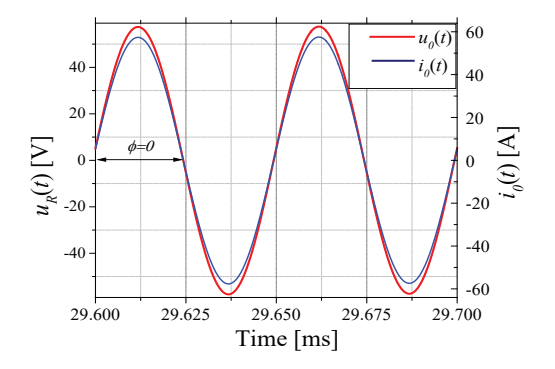


Figure 5. Voltage v0(t) and current  $i_0(t)$  at the same phase  $\phi = 0$ , as a result of resonant condition

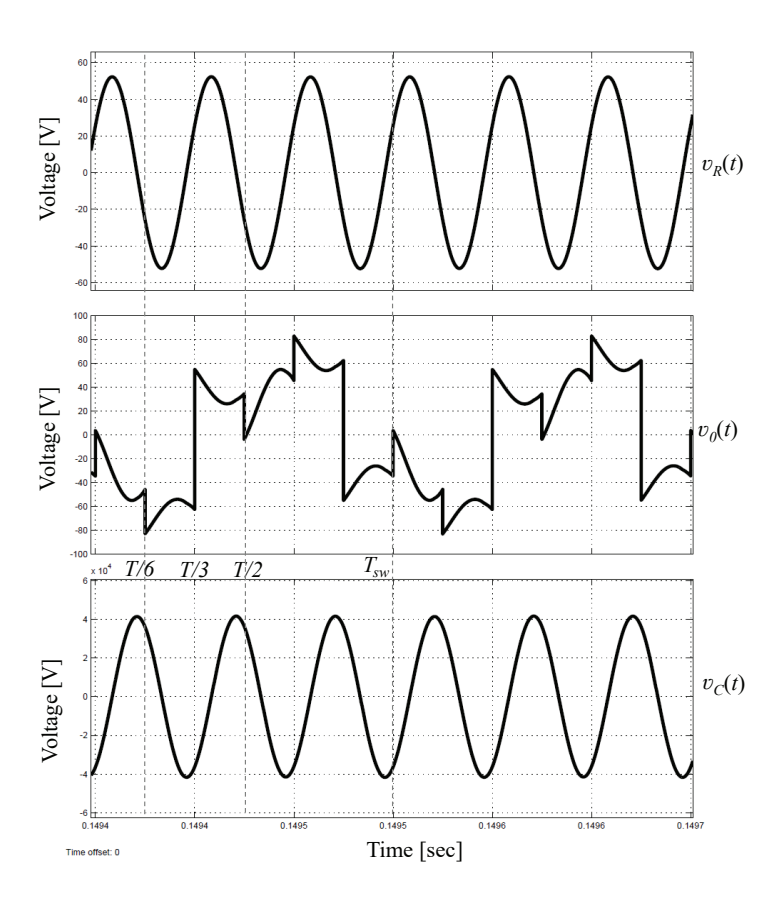


Figure 6. Waveforms of the main voltages  $v_R(t)$ ,  $v_C(t)$  and  $v_0(t)$  in the FB-FCMI

derably reduction of power dissipation in the MOS-FETs. Figure 7b shows the simulation results on instantaneous power  $P_i(t)$  and  $P_{RMS}$  in semiconductors, the RMS value is ~7 mW.

# THE FB-FCMI AT RESONANT MODE: SIMULATION SET-UP

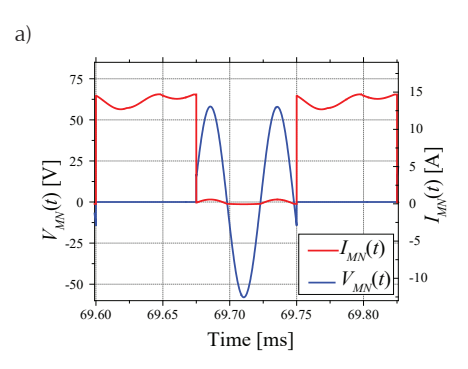
The FB-FMCI showed in Figure 1 is developed and running on SIMULINK/MATLAB® using the SimPowerSystem libraries. In order to get the best performance a previous calculus of *RLC* resonant components either SimPowerSystem or Funtional-Block was made to achieve the best tuning of the resonant condition. The parameter simulation values are; f= 20 kHz, C=10 nF, L=6.333 mH, R =  $1\Omega$  and  $V_M$ =66 V. The simulation parameters on [C1, C1'] and [C2, C2'] are  $V_{DC}$ =200 V,  $V_{C1}$ = $V_{C1}$ '= 133.33 V and  $V_{c2}=V_{c2}'=66.66$  V also the voltage response of flying capacitors are shown in Figure 8a, from this; it is possible to sustain the correct values in open-loop control. Hence, the static inverter gets its natural balance as Meynard and Foch describes in (Meynard et al., 2002). Figure 8b show a detail of voltage  $V_{c2}(t)$  and  $i_{c2}(t)$  current in flying capacitor named C2 working as resonant mode, the ripple voltage  $\Delta v_{C2}(t)$  is about 3.75% of the total voltage  $V_{\text{C2}}(t)$  and  $\Delta i_{\text{C2}}(t)\cong 2.5$  Ap-p, even though the average current throughout C2 estimated by means Origin® is about zero. Then, both C1 and C2 work like an ideal voltage source.

Simulation set-up of a six cell FB-FCMI was designed based on theory of experimental section. Figure 9 shows the voltage in flying capacitors;  $V_{C5}(t)$ =5/6· $V_{DC}$ ,  $V_{C4}(t)$ =4/6 ·  $V_{DC}$ ,  $V_{C3}(t)$ =3/6 ·  $V_{DC}$ ,  $V_{C2}(t)$ =2/6 ·  $V_{DC}$  and  $V_{C1}(t)$ =1/6 ·  $V_{DC}$  considering  $V_{DC}$  = 200 $V_{C1}$ . The natural balance in all cases is getting about  $t_{ss}$ ~0.075 seconds. Moreover, Figure 10 shows an evolution of capacitor voltage  $v_{C}(t)$  expressed as function of  $u_{S3}(t)$ , in these case the output frequency in the element  $V_{C1}(t)$ 0 expressed in so far as the command signal frequency  $v_{C2}(t)$ 1 operates

 $f_{sw} \approx 3.333$  kHz, therefore the statement  $f_0 = N \cdot f_{sw}$ , where N is the number of cell, is substantiated in this work.

# THE FB-FCMI COUPLED TO HIGH VOLTAGE APPLICATION

The high voltage application consists in a proposed tree-cell FB-FCMI coupled to a high voltage transformer where its primary winding inductor is part of the *RLC* resonant-circuit and the secondary winding is cou-



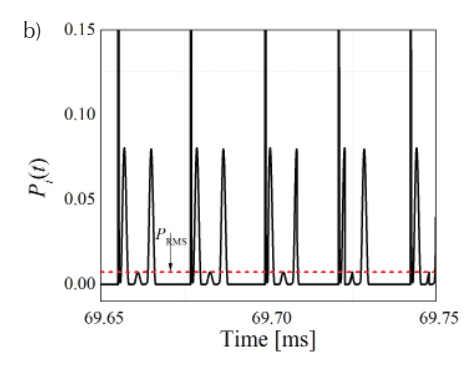
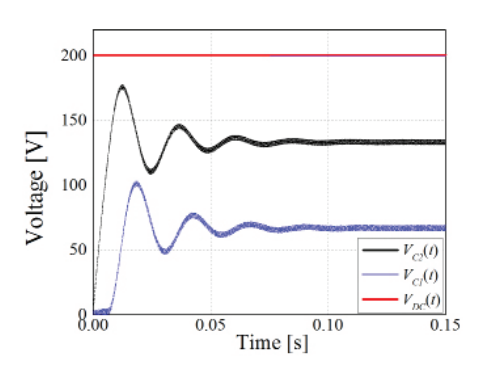


Figure 7. The Zero-Current Switching (ZCS): a) Voltage  $V_{MN}(t)$  and current  $I_{MN}(t)$  through the MOSFET, b) Instantaneous  $P_i(t)$  and  $P_{RMS}$  power behavior



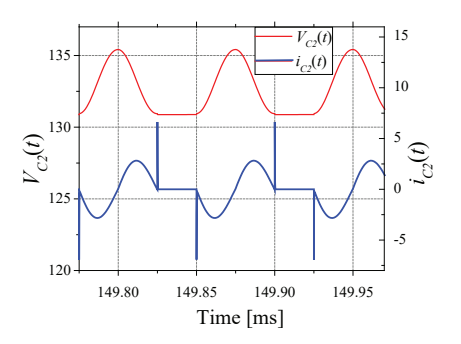


Figure 8. a) Flying Capacitors voltage response  $V_{C1}(t)$  and  $V_{C2}(t)$ , b) Detail of voltage  $V_{C2}(t)$  and current  $i_{C2}(t)$  at resonant mode

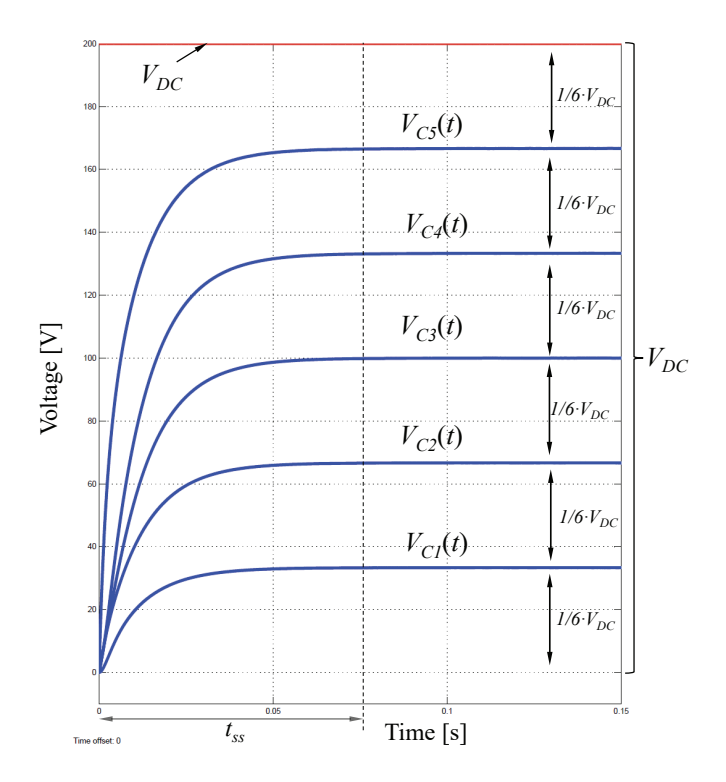


Figure 9. Voltage response in flying capacitors, in a six cell FB-FCMI at resonant mode

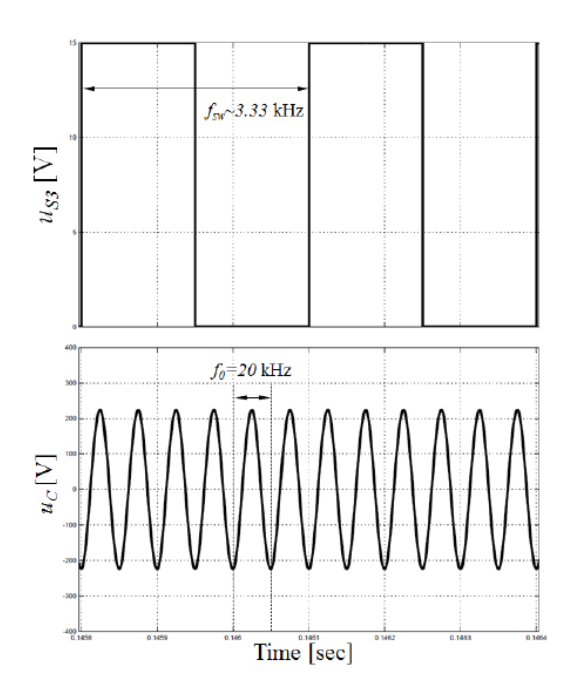


Figure 10. Voltage  $v_R(t)$  operating at  $f_0 = 6 f_{sw}$  expressed as function of  $u_{S3}(t)$  at  $f_{sw}$ 

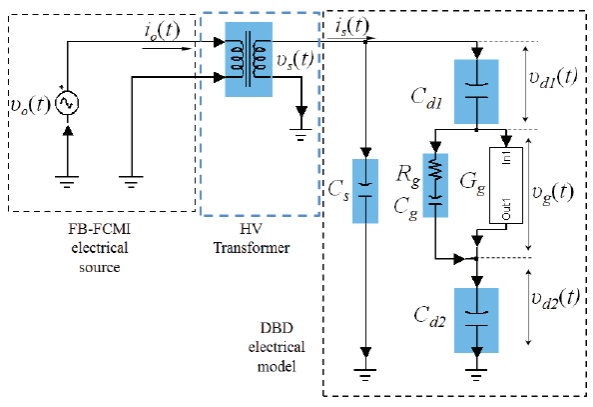


Figure 11. Electrical model of the DBD

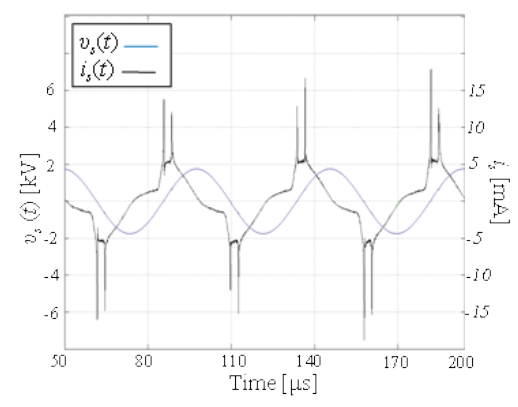


Figure 12. Simulation set-up of DBD in helium

pled an equivalent electrical model of Dielectric Barrier Discharge see Figure 1. The DBD model involves a stray capacitance  $C_s$  due to effect of the capacitance reactor, two dielectric capacitance  $C_{d1}$  and  $C_{d2}$  corresponding to dielectric material as glass, then a parallel circuit is formed; first by a series load  $R_g$ – $C_g$ , and second by a current source controlled by voltage  $V_g$ . Figure 11 shows the schematic and equivalent DBD proposed in (Flores *et al.*, 2009).

The goal of proposed of an electrical model is to provide more information about voltage and current values at the electrical discharge, because in the experimental set-up not only the voltages  $v_d(t)$  and  $v_g(t)$  are not measurable but also parameters are not well known because there are not conventional methods with measurement instruments. Therefore, after simulation processes in SIMULINK/MATLAB® the voltages and currents in the DBD are shown in Figure 12.

Finally, a simulation of DBD running in helium gas and driven by the resonant tree-cell FB-FCMI, which deliver electric power through primary winding towards DBD coupled in the secondary side. Thereby, Figure 12 shows the electrical behavior of voltage  $v_s(t)$  and current  $i_s(t)$  typically in a DBD taking in account literature information in (Flores  $et\ al.$ , 2009) and considering parameters as:

- a) type of ionized gas
- b) applied voltage  $v_s(t)$
- c) current discharge  $i_s(t)$
- d) operation frequency 20 kHz
- e) reactor geometry

In the simulation results voltage  $v_s(t)$  and current  $i_s(t)$  are out of phase because DBD load is predominantly capacitive, as shown in the electrical model of Figure 11. This is an intrinsic characteristic of the electrical DBD behavior; however the system is in resonant mode operation, but the total power consumption by electrical discharge is in the order of units of watts and efficiency is ~20% (Flores *et al.*, 2009).

# Conclusions

The simulation of a FB-FCMI at resonant mode is presented. The command control generates twelve signals at Fundamental Frequency strategy operating, at  $f_{sw} = f_0/N$ , where N is the total number of cells in the static inverter. The statement about relation between output frequency and commutation frequency is given by  $f_o = N \cdot f_{sw}$ , in this work in order to validate that condition from this kind of power static inverter, not only a three-

cell flying capacitor inverter was designed but also a six-cell inverter was simulated. So, the natural balance of the voltage in flying capacitors at open-loop control in both cases is correct achieved. The *RLC* passive elements are designed based on the resonance frequency which is the same that the output inverter frequency which is the same that the output inverter frequency  $f_0$ =20 kHz, hence optimal coupling between *RLC* and FB-FCMI was successfully set-up simulated in MAT-LAB®. Because of resonant condition, the semiconductor devices operate at ZCS mode properly, so the dv/dt snubber circuit protection is reduced in its size. Finally a full system conformed by FB-FCMI coupled at DBD electrical model is running on SIMULINK/MATLAB® in order to prove the high voltage application to generate electrical discharges in helium gas.

### **AKNOWLEDGEMENTS**

The authors wish to thank COMECYT for financial support and M.R.S. Sámano-Ángeles Antonio director of the Centro Universitario UAEMex Atlacomulco.

# REFERENCES

- Aguillón-García J., Fernández-Nava J.M., Bañuelos-Sánchez P. Unbalanced volage effects on a single phase multilevel inverter due to control strategies, 26<sup>th</sup> Annual International Telecommunications Energy Conference INTELEC 2004, volume 19, Chicago, EU, September 2004, pp. 140-145.
- Abu-Rub H., Holtz J., Rodriguez J. Medium-Voltage Multilevel Converters: State of the Art, Challenges, and Requirements in Industrial Applications. *IEEE Transactions on Industrial Applications*, volume 57 (issue 8), 2010: 2581-2596.
- Fernao-Pires V., Martins J.F., Foito D., Chen H. A grid connected photovoltaic system with a multilevel inverter and a Le-Blanc transformer. *International Journal of Renewable Energy Research*, volume 2 (issue 2), 2012: 84-91.
- Flores-Fuentes A.A., Peña-Eguiluz R., López-Callejas R., Mercado-Cabrera A., Valencia-Alvarado R., Barocio-Delgado S., De la Piedad-Beneitez A. Electrical model of an atmospheric pressure dielectric barrier discharge cell. *IEEE Transaction on Plasma Science*, volume 37 (issue 1), 2009: 128-134.

- Hirofumi A. The state-of-the-art of power electronics in Japan. *IEEE Transactions on Power Electronics*, volume 13 (issue 2), 1998: 345-356.
- Holmes D. and Lipo T. *Pulse width modulation for power converter: Principles and practice*, 1<sup>st</sup> ed., Piscataway, NY, IEEE Press Wiley, 2003, pp. 600-724.
- López-Fernández J.A., Peña-Eguiluz R., *Member, IEEE*, López-Callejas R., Mercado-Cabrera A., Jaramillo-Sierra B., Rodríguez-Méndez B., Valencia-Alvarado R., Muñoz-Castro A.E. A 10- to 30-kHz adjustable frequency resonant full-bridge multicell power converter. *IEEE Transactions on Industrial Electronics*, volume 62 (issue 4), 2015: 2215-2223.
- Loren L. New power semiconductor components for future innovate high frequency power converters, IEEE International Conference on Industrial Technology, volume 2, Maribor, Slovenia, December 2003: 1173-1177.
- Meynard T.A., Foch H., Thomas P., Courault J., Jakdo R., Nahrstaedt M. Multicell Converters: Basic Concepts and Industry Applications. *IEEE Transactions on Industrial Electronics*, volume 49 (issue 5), 2002: 955-964.
- Péña-Eguiluz R., López-Fernández J.A., Mercado-Cabrera A., Jaramillo-Sierra B., López-Callejas R., Rodríguez-Méndez B., Valencia-Alvarado R., Flores-Fuentes A.A., Muñoz-Castro A.E. *Plasma Science and Technology*, volume 19, 2017: 1-10.
- Rodriguez J., Jih-Sheng L., Fang-Zheng P. Multilevel inverters: a survey of topologies, controls, and applications. *IEEE on Industrial Electronics*, volume 49 (issue 4), 2002: 724-738.
- Rodríguez J., Kazimierkowski M.P., Espinoza J.R. State of the art of finite control set model predictive control in power electronics. *IEEE Transactions on Industrial Informatics*, volume 9 (issue 2), 2012: 1003-1016.
- Samir K., Malinowski M., Gopakumar K.Recent advances and industrial applications of multilevel converters. *IEEE on Industrial Electronics*, volume 57 (issue 8), 2010: 2553-2580.
- Tolbert L.M., Peng F.Z. Multilevel converters as a utility interface for renewable energy systems. Power Engineering Society Summer Meeting, 16-20 July 2000, Seattle WA, USA.
- Zhe C., Guerrero J.M., Blaabjerg F. A Review of the state of the art of power electronics for wind turbines. *IEEE Transactions on Power Electronics*, volume 24 (issue 8), 2009: 1859-1875.

### Suggested citation:

### Chicago style citation

Flores-Fuentes, Allan Antonio, José Arturo Pérez-Martínez, Juan Fernando García-Mejía, Iván Osvaldo Rossano-Díaz, Carlos Eduardo Torres-Reyes. Design and simulation of a resonant full-bridge multicell power inverter for high-voltage applications. *Ingeniería Investigación y Tecnología*, XIX, 03 (2018): 245-254.

### ISO 690 citation style

Flores-Fuentes A.A., Pérez-Martínez J.A., García-Mejía J.F., Rossano-Díaz I.O., Torres-Reyes C.E. Design and simulation of a resonant full-bridge multicell power inverter for high-voltage applications. *Ingeniería Investigación y Tecnología*, volumen XIX (issue 3), July-September 2018: 245-254.

### **ABOUT THE AUTHORS**

Flores-Fuentes Allan Antonio. Ph. D. degree in electronics engineering by Instituto Tecnológico de Toluca, México, 2009. Since 2011, he has been working in the Universidad Autónoma del Estado de México. His research interest includes multilevel static converters applied to industrial applications, pulsed power supplies and instrumentation and control systems.

Pérez-Martínez José Arturo. Ph.D. degree in Electronic engineering from the Instituto Tecnológico de Toluca, Toluca, Mexico, since 2010. His research concerns in static RF converter applied to plasma micro-discharges in different configuration reactors and control systems, also the automation of advanced manufacturing processes. He is working in the Universidad Autónoma del Estado de México, Centro Universitario UAEM Atlacomulco, México.

García-Mejía Juan Fernando. Received the title of Engineer in Electronics from the Instituto Tecnológico de Toluca in 2004, he obtained the degree of Master of Science in Electronics by the same institution. Since 2004 he has been working at the Centro Universitario UAEM Atlacomulco, where he is a full-time professor with PRODEP profile and leader of the academic group "Software Development, Devices and Systems Applied to the Technological Innovation", his research line is focused on the development of virtual instruments and the use of softcomputing techniques applied to control engineering.

Rossano-Díaz Iván Osvaldo. M.A. Engineer in electronics by Instituto Tecnológico de Toluca, México, 2004. Since 2009, he has been with the Universidad Autónoma del Estado de México, where he is currently a Reacher. His research interest include Sliding control, Digital control, static converters and control applied to Bioelectronics Systems.

Torres-Reyes Carlos Eduardo. B.Sc. degree in electronic engineering from the Instituto Tecnológico de Toluca, Toluca, Mexico, in 2002, also he received the Ph.D. degree in the same institution in 2010. Actually he works in the C.U. Atlacomulco of the Universidad Autónoma del Estado de México, in developing of plasma torch power supply and associated electronic devices.